Development of Propulsion Testing and Integration Facilities at Canon Electronics

IEPC-2019-A796

Presented at the 36th International Electric Propulsion Conference
University of Vienna, Austria
September 15-20, 2019

Kento Masuyama,* Waku Hatakeyama,† Masanobu Mizukawa,‡ and Shunya Morita§
Canon Electronics Inc., Minato-ku, Tokyo 105–0011, Japan

Canon Electronics is expanding on its satellite bus capabilities following the success of CE-SAT-I. One enabling technology that has been identified is electric propulsion. Electric propulsion allows for more flexible launches, constellation phasing, end-of-life deorbiting, and orbit maintenance even at low altitude. Many new and old space companies now offer commercial off-the-shelf electric propulsion modules, but many do not have the flight heritage and extensive testing demanded by traditional aerospace customers. Furthermore, with increasing number of technologies and providers, a satellite manufacturer must be able to offer the most advanced options while protecting itself from risks in future component availability. In order to meet these demands, Canon Electronics has begun developing a vacuum chamber testing facility for rapid testing and iteration of new propulsion systems and their integration with the CE-SAT bus. The chamber is designed for flexible testing with shields and beam dump for mitigating material compatibility and back sputtering. Initial capabilities will include direct thrust measurement and scanning Faraday cup beam probe.

I. Introduction

Canon Electronics (CE) entered the small satellite and Earth observation fields in 2017 with the launch of CE-SAT-I, a 65 kg in-house developed microsatellite with 0.9 m ground sampling distance (GSD) capability. After two years of successful operations with CE-SAT-I and valuable insight into improved system design and concept of operations for realizing CE's business strategy, electric propulsion (EP) has been identified as a key enabler for future CE-SAT missions. CE envisions an Earth observation constellation consisting of satellites with telescopes ranging from CubeSat-size to 40 cm in diameter and possibly larger, fitted with high sensitivity sensors for low-light imaging. The addition of propulsive capabilities to these satellites will increase launch opportunities, allow station keeping in very low orbits for increased ground resolution, ensure proper orbit phasing, and provide deorbiting capabilities for debris and congestion mitigation.

Electric propulsion options for microsatellites have seen rapid growth in recent years, with both traditional propulsion providers and startups bringing new products to market.[1,2] These propulsion systems are based on technologies with a wide range of maturity, including miniaturized versions of classical electric propulsion systems as well as novel concepts. Many of these make use of new propellants which offer several advantages over hydrazine or xenon. Iodine, tested with hall thrusters[3] and gridded ion thrusters,[4,5] can be stored as a solid thereby increasing density and reducing risk due to high pressure storage. Liquid metal ion sources including indium[6] and gallium[7] are even denser metals and allow for safer handling on ground during integration and testing. Liquid propellants also offer higher density than gases, with ionic liquid ion sources offering negligible vapor pressures for low-pressure storage[8] and water promising future refuelling via in-situ

*Senior Researcher, Satellite Systems Laboratory, masuyama.kento@canon-elec.co.jp
†Satellite Systems Laboratory, hatakeyama.waku@canon-elec.co.jp
‡Satellite Systems Laboratory, mizukawa.masanobu@canon-elec.co.jp
§Satellite Systems Laboratory, morita.shunya@canon-elec.co.jp

resource utilization.[9,10] Many of these materials are commonly available and offer significant savings in cost, an important consideration for small satellite missions and large constellations.

To provide a satellite system capable of adapting to new and changing requirements, it is important to iterate and test rapidly. In today's environment with numerous and ever-increasing players in fierce competition, satellite integrators must ensure that critical performance can be recovered by alternate technologies in case externally supplied components become unavailable. With so many new technologies offering high performance and relatively low cost at the expense of limited flight heritage, it is a strong advantage to have access to adequate testing facilities to verify component-level performance as well as proper integration with the bus. Independent testing of candidate propulsion systems increases confidence in their application for future missions and products. Extensive testing capabilities also opens the door for potential collaborations with new propulsion system providers, for ground and in-orbit testing. To meet such needs, CE is currently in the process of developing a vacuum testing facility with tools for measuring thrust, thrust vector, beam divergence, and electrical connectivity with the bus and onboard computer. This paper describes the facilities for testing of propulsion-enabled micro and nanosatellites and presents the expected performance increase compared to the CE-SAT-I baseline.

II. Test Chamber

A new vacuum chamber, shown in Fig. 1, has been designed for thruster firing tests. The size of the vacuum chamber is $2.1\,\mathrm{m} \times 2.25\,\mathrm{m} \times 2.95\,\mathrm{m}$. The vacuum chamber has a 20 inch cryogenic pump whose pumping capacity is $9000\,\mathrm{L\,s^{-1}}$ (Ar) to handle smaller propulsion systems, and an auxiliary 20 inch port is available for future expansion. Twelve NW-40 and two NW-50 ports can be used for transferring command and data signals, electrical power, and fluids into or out of the chamber. The chamber is also equipped with removable shields for protecting the chamber walls from non-gaseous propellants such as ionic liquids, liquid metals, or especially corrosive materials like iodine. The pump ports are protected by separate shield panels so that conductance is maintained into the main testing cavity, but no line-of-sight access is possible into the pump from any chamber walls. A beam dump is planned to be installed on the downstream flange so that sputtered particles do not head directly toward the test equipment and EP system. Due to the high specific impulse found in many EP systems, significant sputtering is expected at the beam dump and shields — this requires tuning of the materials to maintain compatibility and also tuning of the geometry with consideration of sputtering yield. The shields and the beam dump are thus designed to be easily removable so that appropriate materials and geometry may be selected per combination of thruster and propellant.

In order to install experiments easily into the vacuum chamber, mouting rails are equipped inside the vacuum chamber. The experimental setup will be mounted on a mounting cart and pushed into the vacuum chamber along the mounting rails. The mounting rails are fixed to a leveling system which can be adjusted independent of chamber walls; this allows to counter future shifts in ground level due to chamber weight or earthquakes. $1.61\,\mathrm{m} \times 1.35\,\mathrm{m} \times 2.23\,\mathrm{m}$ is available after installing chamber shields, beam dump, and mouting cart. Therefore, there is enough space for CE-SAT-I with an additional $1.35\,\mathrm{m}$ downstream to avoid excessive sputtering. A clean tent, which is better than class ISO 8, is planned to be installed over the entrance of the vacuum chamber for preparation of experiments.

III. Test Equipment

From a satellite integration perspective, the physics of the propulsion system may be treated as a black box. Instead, the key parameters to be verified are in performance and interactions with the rest of the spacecraft. For performance, thrust magnitude and accuracy affect mission planning. Also the total impulse is necessary in order to satisfy the Δv budget for the mission. More practically, the specific impulse can be calculated from thrust data and mass flow rate, or in case the mass flow rate cannot be accessed in an enclosed propulsion system, beam current. The total impulse is then calculated as the product with total propellant mass.

For interactions and interfaces, power consumption and heat output play large parts, especially in small satellites. If the mission requires a large amount of total impulse, changes in mass, center of gravity, and moment of inertia may become significant. The quality of mechanical and electrical connections to the bus are important, as shifts in the mounting angle can introduce thrust vector errors and poor electrical grounding may lead to differential charging and dangerous discharge events. The thruster plume also warrants study, as

Figure 1. Vacuum chamber appearance

impingement on spacecraft surfaces cause anomalous torques and potential damage to photovoltaics, optical surfaces, and antennae.[11] Current density distribution in the plume can also be a way to determine thrust vector alignment errors,[12] which may lead to thrust magnitude errors and anomalous torques if unaccounted for.

The vacuum chamber presented above is large enough for short duration tests of EP systems integrated on a CE-SAT-I size ($50\,\mathrm{cm} \times 50\,\mathrm{cm} \times 85\,\mathrm{cm}$) bus, allowing characterization of electrical and thermal connections. This also allows for testing of C&DH compatibility with representative cable harnesses, as some commands to the thruster cannot be fully tested in atmosphere due to high voltages, propellant flow, or high temperatures. Additional facilities on premises allow for non-vacuum integration tests such as vibration, shock, electromagnetic interference (EMI), and thermal cycling. Furthermore, tools for measuring thrust and beam distribution are under development. These will be conducted at component-level to reduce loads on the thrust stand and actuators.

A. Thrust Stand

For small EP systems, weight is often a much larger force than the produced thrust. In order to accurately measure the thrust, the effect of gravity must be reduced. Torsional balance thrust stands are ideally not affected by gravity in measuring the thrust[13] due to the thrust-generated torque acting perpendicular to gravity. The thrust stand developed at CE, as shown in Fig. 2, has a horizontal beam and pivots at the center of the beam. A thruster is located at one end of the beam, and a counterweight system and a copper plate for damping are located at the other end. The flexural pivots are torsion springs, displaced only by torques in a specific geometric plane. In order not to stress the pivot, the beam is required to be lightweight and rigid — this is accomplished with a U-shaped Aluminum beam. In a torsional balance type thrust stand, the beam is only supported by the pivot at the center. In order to stabilize the beam, coaxial pivots are placed above and below the beam. When a torsional balance thrust stand has two or more pivots, the alignment error between those pivots can inhibit the effect of the torsion spring. A coaxial alignment of less than $\phi 0.2\,\mathrm{mm}$ was achieved between the two pivots via high machining accuracy.

The counterweight system is adjusted to place the total beam center of gravity at the pivot centerline, so that the effect of misalignment between the rotation axis and gravity is minimized.[14] In order to precisely adjust the center of gravity, the counter weight is placed on a small linear stage attached to the beam. This system also allows for the thrust balance to work with different thrusters within the mass tolerance.

In order to reduce vibrations from change of the thrust force or from external noise, an eddy current damper has been implemented.[15] When a metal moves within a strong magnetic field, electric currents flow in the metal and a resulting electromagnetic force in opposition to the motion acts on the metal. Damping effort depends on the moment of inertia of the thrust stand, which in turn depends on the thruster under study. The eddy current damper's damping effort can be changed by changing the copper plate thickness.

Thrust is calculated from the amount of movement of the end of the beam. When a thrust force is added to the beam, the beam rotates around the pivots and stops at an equilibrium position. The horizontal one-axis movement of the beam is measured by a laser sensor. The relation between the travel distance of the beam and the torque added to the beam should be calibrated before and/or after each test. In order to add known torques to the beam, a string, pulley, and weights are used. One side of the string is fixed at a hole on the beam. There are three holes at different arm lengths along the beam as options to calibrate different ranges of thrusts. The other side of the string has some weights and is passed over a pulley in order to convert the vertical weight force to horizontal. Tension in the string is changed by scooping up the weights using a vertically moving linear stage. The thrust stand can measure thrust from 0 to 40 mN, and thrusters or clusters of thrusters with total mass up to 10 kg can be supported. 26 electrical wires (including 5 pairs of thermocouple wires) are on the beam and connect with the outside of the thrust stand beam. The wires on the beam are gathered near the center of the beam in order to lessen the anomalous torque noise from their tension, and extend upwards to the fixed portion of the thrust stand.

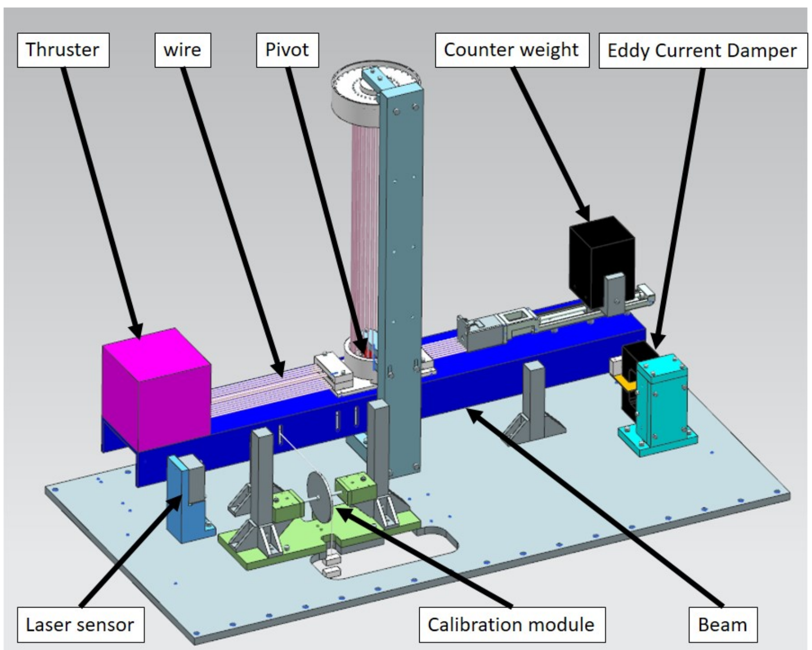

Figure 2. The thrust stand CAD model

B. Beam Diagnostics

A Faraday cup is an instrument used for direct current density measurement inside a plasma. It is possible to measure the plasma plume distribution of EP systems and current density at multiple points inside the plume. In previous studies, the plume distribution has been used for investigating thruster physics,[16] avoiding satellite sputtering or contamination by the plume,[17] and measuring the thrust vector.[18] In general, a Faraday cup consists of a collector electrode that is dedicated for current measurement and one or more grids for eliminating measurement errors.

It is required to consider the following errors when making reliable measurements of current density:

1. Secondary electron emission

2. Charge exchange effect

3. Probe material back sputtering

Secondary electron emission and charge exchange effects cause errors on the current measurement. Probe material back sputtering can lead to non-nominal operation of the thruster undergoing study. A Faraday cup is designed to eliminate the effects of these two errors. Future development includes eliminating the charge exchange effect.

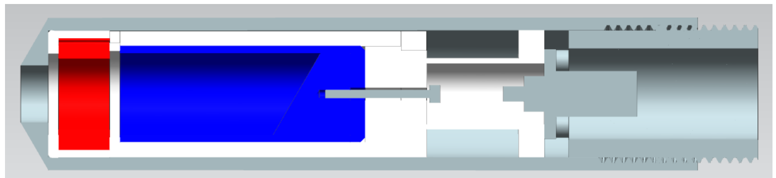

Figure 3. The cross section of the Faraday cup

Fig. 3 shows the cross section of the Faraday cup. The blue part is the collector responsible for ion current collection. This part connects to a Keithley picoammeter located outside the chamber. The area of the orifice located on the left end of the Faraday cup is $100\,\mathrm{mm}^2$, and the current density can be calculated by dividing the collector current by the orifice area. The ion hitting area of the collector is inclined by 60° with respect to the main axis of the Faraday cup to reduce the escaping secondary electrons geometrically.[19] It is assumed that this design also contributes to reducing the probe material back sputtering, because typically most part of the sputtered materials are scattered in the opposite direction of the incident direction.[20] The red part is a negative potential grid to suppress secondary electron emission from the collector. Secondary electrons are generated by high energy ion bombardment, and the resulting electron current leaving the collector appears as a positive shift in the measured current. Grid voltage can be tuned depending on the thruster. The white parts are PTFE insulators for isolating high voltage components from high potential parts. The front surface of the probe also has an inclination of 60° with respect to the primary ion beam so that the back sputtering materials do not head directly towards the thruster.

Two dimensional plume measurement will be acquired using a rotation stage and a goniometer stage. The Faraday cup will be connected to a swing arm, which is exchangeable depending on ion current density, mounted on a rotation stage, which enables scanning the ion density horizontally from 0° to 180°. The rotation axis of the stage passes through the thrust origin, for example the center of the outermost grid on a gridded thruster. A goniometer stage is similar to rotation stages but can rotate an object about a fixed point external to the mounting stage. The thruster will be mounted on the goniometer such that it rotates vertically about its thrust origin. By using the two stages, the thrust vector offset from its nominal alignment to the thruster body frame can be measured.

C. Additional Facilities

In addition to the vacuum testing facility, CE's satellite and component testing facilities include a number of equipment and resources. Two vibration test rigs allow for natural frequency determination and random vibration testing in all axes. A shock test stand is under development to satisfy most launch provider requirements. A thermal vapor deposition system has been converted into a chamber for analyzing material properties such as thermal conductivity. Three temperature chambers allow for thermal cycling tests, with the smallest appropriate for individual small satellite components and the medium and large chambers large enough for integrated satellites. Finally, an anechoic chamber roughly $11\,\mathrm{m} \times 5\,\mathrm{m} \times 5\,\mathrm{m}$ in size allows EMI testing and characterization of communications and other radio frequency systems.

IV. Effect on Satellite Performance

The necessity of propulsion systems on low Earth orbit satellites and constellations for station-keeping, orbit raising, phase changes, and deorbit have been discussed in literature.[21–23] As an Earth observation satellite operator, another attractive application of electric propulsion is in very low altitude flight. Optical resolution improves linearly with both altitude h and telescope diameter D as

$$GSD = \frac{h l_{sensor}}{f p_{sensor}} \tag{1}$$

$$\Delta\ell = \frac{h\lambda}{D} \tag{2}$$

where l_{sensor} and p_{sensor} are characteristic length and pixel count of the imaging sensor, f is focal length, and $\Delta\ell$ is spatial resolution. As mass is a key consideration for satellite launch and thus lifetime cost, and the payload mass can be expected to increase as $\propto D^3$, it is far more efficient to decrease altitude than increase diameter. At altitudes below 400 km, atmospheric drag is significant and must be counteracted in order to keep the satellite from reentry and disintegration. Such maneuvers have been demonstrated with gridded ion engines by the GOCE[24] and SLATS[25] missions.

Using a simple exponential model for atmospheric density and coefficient of drag $c_D = 2$,[26] the magnitude of drag force on a CE-SAT-I size satellite is shown in Fig. 4.

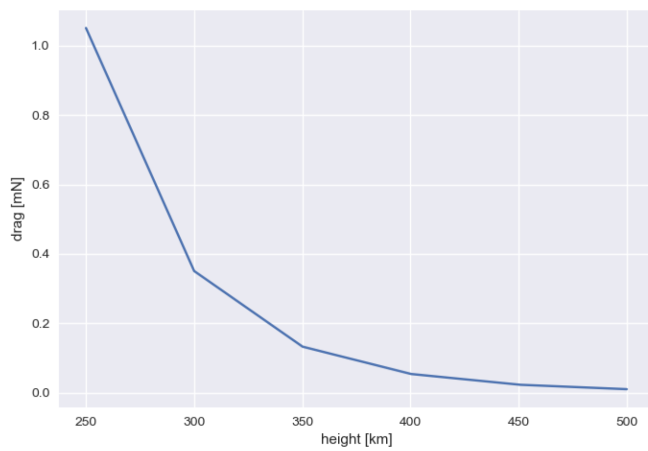

Figure 4. Drag on a microsatellite at low altitude

For example, at an altitude of 300 km, an average thrust of 0.35 mN should allow zero-drag flight. Using Eq. 1 and a reference GSD of 0.9 m at 500 km for CE-SAT-I, the same payload will give a GSD of 0.54 m at 300 km. Fig. 5 and Fig. 6 show what this improvement looks like, with simulated images. The main features like individual cars are resolved in both images; however, the smaller GSD image shows significant improvement in details such as parking lot lines and number of pedestrians.

Figure 5. GSD 0.9 m

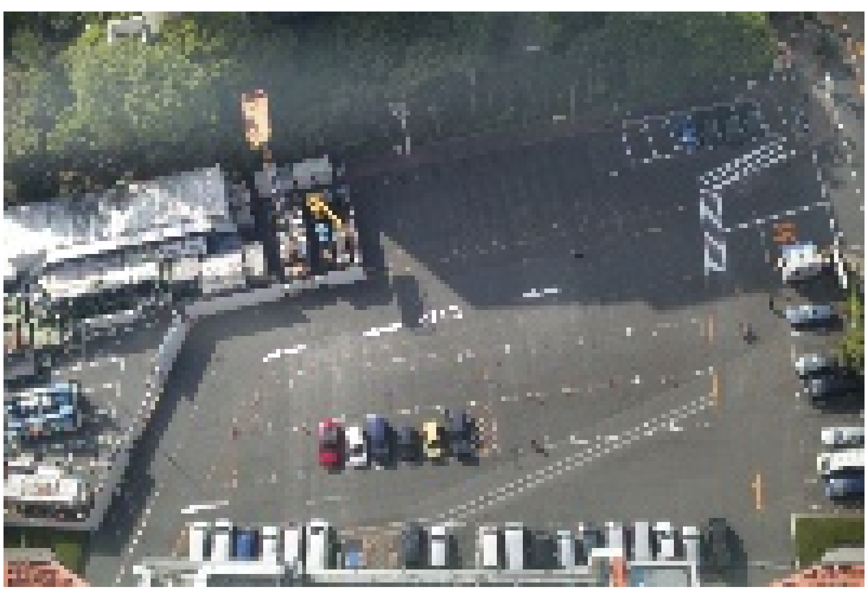

Figure 6. GSD 0.54 m

V. Conclusion

CE has developed a vacuum testing facility for unit and integration testing of EP systems on small satellites. The chamber is designed for rapidly testing different propulsion systems and can be set up for various propellant options. Diagnostics being designed and manufactured include direct thrust measurement and Faraday cup beam probe. This chamber, in addition to other satellite test facilities available at CE, allows for quick iterations of bus integration and testing to better meet customer needs and allow fallback options in case product availability becomes an issue. Furthermore, high specific impulse thrust allows for Earth observation missions in very low altitude by counteracting atmospheric drag. This enables a more efficient increase in ground resolution than increasing optics size. The vacuum testing facility is scheduled to be fully operational in 2019, with validation tests and first tests of candidate propulsion modules before the end of the year.

References

[1]Lev, D., Myers, R. M., Lemmer, K. M., Kolbeck, J., Keidar, M., Koizumi, H., Yu, D., Schoenherr, T., Gonzalez, J., Choe, W., Albertoni, R., and Hart, W., "The Technological and Commercial Expansion of Electric Propulsion in the Past 24 Years," *35th International Electric Propulsion Conference*, 2017.

[2]Levchenko, I., Bazaka, K., Ding, Y., Raitses, Y., Mazouffre, S., Henning, T., Klar, P. J., Shinohara, S., Schein, J., Garrigues, L., Kim, M., Lev, D., Taccogna, F., Boswell, R. W., Charles, C., Koizumi, H., Shen, Y., Scharlemann, C., Keidar, M., and Xu, S., "Space micropropulsion systems for Cubesats and small satellites: From proximate targets to furthermost frontiers," *Applied Physics Reviews*, Vol. 5, No. 1, 3 2018.

[3]Jehle, M. and L, A., "Iodine Small Satellite Propulsion Demonstration – iSAT," *31st Annual AIAA/USU Conerence on Small Satellites*, 2017.

[4]Tsay, M., Model, J., Barcroft, C., Frongillo, J., Zwahlen, J., and Feng, C., "Integrated Testing of Iodine BIT-3 RF Ion Propulsion System for 6U CubeSat Applications," *35th International Electric Propulsion Conference*, 2017.

[5]Rafalskyi, D. and Aanesland, A., "A Neutralizer-Free Gridded Ion Thruster Embedded Into A 1U Cubesat Module," *35th International Electric Propulsion Conference*, 2017.

[6]Seifert, B., Buldrini, N., Hörbe, T., Plesescu, F., Reissner, A., Krejci, D., Friedhoff, P., and Lai, S., "In-orbit Demonstration of the Indium-FEEP IFM Nano Thruster," *6th Space Propulsion Conference*, 2018.

[7]Bock, D. and Tajmar, M., "Highly miniaturized FEEP propulsion system (NanoFEEP) for attitude and orbit control of CubeSats," *Acta Astronautica*, Vol. 144, No. 9, 3 2018, pp. 422–428.

[8]Krejci, D., Mier-Hicks, F., Fucetola, C., and Lozano, P., "High efficiency ionic liquid electrospray propulsion for Nanosatellites," *67th International Astronautical Congress*, 2016.

[9]Nakagawa, Y., Koizumi, H., Kawahara, H., and Komurasaki, K., "Performance characterization of a miniature microwave discharge ion thruster operated with water," *Acta Astronautica*, Vol. 157, 4 2019, pp. 294–299.

[10]Koizumi, H., Asakawa, J., Nakagawa, Y., Nishii, K., Takao, Y., Nakano, M., and Funase, R., "Assessment of Micropropulsion System Unifying Water Ion Thrusters and Water Resistojet Thrusters," *Journal of Spacecraft and Rockets*, 2019.

[11]Corey, R. L. and Pidgeon, D. J., "Electric Propulsion at Space Systems/Loral," *31st International Electric Propulsion Conference*, 2009.

[12]Clark, S. D. and Stapleton, A. W., "Development and Commissioning of an Electric Propulsion Test Facility," *Joint Conference of 30th International Symposium on Space Technology and Science, 34th International Electric Propulsion Conference, and 6th Nano-satellite Symposium*, 2015.

[13]Pancotti, A., Haag, T., King, S., Walker, M., Polk, J. E., Pancotti, A., Haag, T., King, S., Walker, M., Blakely, J., and Ziemer, J., "Recommended Practices in Thrust Measurements," *33rd International Electric Propulsion Conference*, 2013.

[14]Ziemer, J. K., "Performance Measurements Using a Sub-Micronewton Resolution Thrust Stand," *27th International Electric Propulsion Conference*, 2001.

[15]Nagaya, K. and Kojima, H., "Shape Characteristics of a Magnetic Damper Consisting of a Rectangular Magnetic Flux and a Rectangular Conductor," *Bulletin of the JSME*, Vol. 25, No. 206, 8 1982.

[16]Brown, D. L. and Gallimore, A. D., "Evaluation of Facility Effects on Ion Migration in a Hall Thruster Plume," *Journal of Propulsion and Power*, Vol. 27, 2011, pp. 573–585.

[17]Ekholm, J. M., Hargus, W. A., Larson, C. W., Nakles, M. R., Reed, G., and Niemela, C. S., "Plume Characteristics of the Busek 600 W Hall thruster," Tech. Rep. July 2006, 2006.

[18]Pagano, D., Coduti, G., Scaranzin, S., Meniconi, G., Scortecci, F., and Kutufa, N., "Performance of Plume Characterization of the SPT100-B Thruster," *IEPC2015*, 2015, pp. 1–15.

[19]Harasimowicz, J. and Welsch, C. P., "Faraday Cup for Low-Energy , Low-Intensity Beam Measurements at the USR," *Cockcroft Institute*, 2009, pp. 4–6.

[20]Williams, J., Johnson, M., and Williams, D., "Differential Sputtering Behavior of Pyrolytic Graphite and Carbon-Carbon Composite Under Xenon Bombardment," 2004, pp. 1–21.

[21]Myers, R. M., Oleson, S. R., Curran, F. M., and Schneider, S. J., "Small Satellite Propulsion Options," *30th Joint Propulsion Conference*, 1994.

[22]Martinez-Sanchez, M. and Pollard, J. E., "Spacecraft Electric Propulsion—An Overview," *Journal of Propulsion and Power*, Vol. 14, No. 5, 9 1998, pp. 688–699.

[23]De Weck, O. L., De Neufville, R., and Chaize, M., "Staged Deployment of Communications Satellite Constellations in Low Earth Orbit," *Journal of Aerospace Computing, Information, and Communication*, Vol. 1, No. 3, 3 2004, pp. 119–136.

[24]Romanazzo, M., Steiger, C., Sechi, G., Saponara, M., Rezazad, M., Nino, A. P., Costa, A. D., Fehringer, M., Floberghagen, R., André, G., and Pier, P., "In-Orbit Experience With the Drag-Free Attitude and Orbit Control System of ESA's Gravity Mission GOCE," *Proceedings of the 8th International Conference on Guidance, Navigation and Control*, , No. 6, 2011, pp. 1–17.

[25]Hoshino, H., Konoue, K., Kaneko, Y., and Sasaki, M., "Regional Observation by Super Low Altitude Test Satellite "TSUBAME" (SLATS)," *Journal of the Japan society of photogrammetry and remote sensing*, Vol. 56, No. 5, 2017, pp. 248–251.

[26]Panwar, R., "Satellite Orbit Decay Calculations," Tech. rep., The Australian Space Weather Agency, 1999.